USING FINITE ELEMENTS MODEL OF THE HUMAN BODY FOR SHAPE OPTIMIZATION OF SEATS: OPTIMIZATION MATERIAL PROPERTIES

Niels C.C.M. Moes and Imre Horvath

Keywords: ergonomics, finite elements Model, shape conceptualization, pressure distribution, ischial tuberosities, optimisation

1. Introduction

CAD programs are often used to design the shape of a product. Unfortunately such programs are not equipped to evaluate the product for design concepts such as ergonomics, manufacturability, aesthetics. Even less is it possible to balance these concepts in design decisions or in design optimization. It is the aim of the Integrated Concept Advancement (ICA) project [Horv´ath 1998] to develop an Intelligent Balanced Comprehension Engine for assembling and synthesizing the knowledge of such design concepts in product design proposals. The current subproject explores the implementation of ergonomics knowledge, rules and guidelines in such a system. Since a vast amount of valuable ergonomics knowledge was created during the last century, a general comprehension is virtually impossible, necessitating a convergence of focus. We concentrated on the ergonomics aspects of the shape of the contact area of physically handled products, in particular on the transmission of the interactive force between a seat and the body, resulting in a pressure distribution, and on the physiological criteria for pressure exertion.

A design aid as described above would be a great benefit for that area of conceptual design, where physiological functioning of the skin and its underlying tissues are strongly related with the shape of the contact area. Unfortunately such 'analytical' solutions have not yet been developed, so that we have to apply optimization techniques.
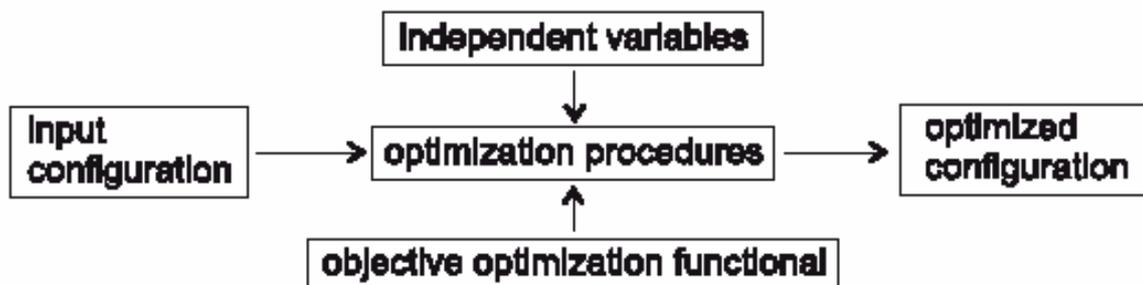

Figure 1. The input configuration is optimized by modification of the input variables for improving the objective optimization functional

1.1 Optimization

A typical general optimization procedure is shown in figure 1. It consists of (i) an object to be modified, which is called the *input configuratio*n, (ii) a variable to control the optimization, or the *objective optim-ization functiona*l, (iii) a (set of) object-quantity(ies) that will actually be varied, called the *independent variable*s,and (iv) the resulting modified configuration. The object to be modified is the part of the hu-man body that is involved in sitting. The control variable to be optimized, which is usually called the *objective optimization functional* is the *Ergonomics Goodness Inde*x,(E). The independent variables is the pressure distribution in the contact area. The modified configuration is the body with the modified properties.
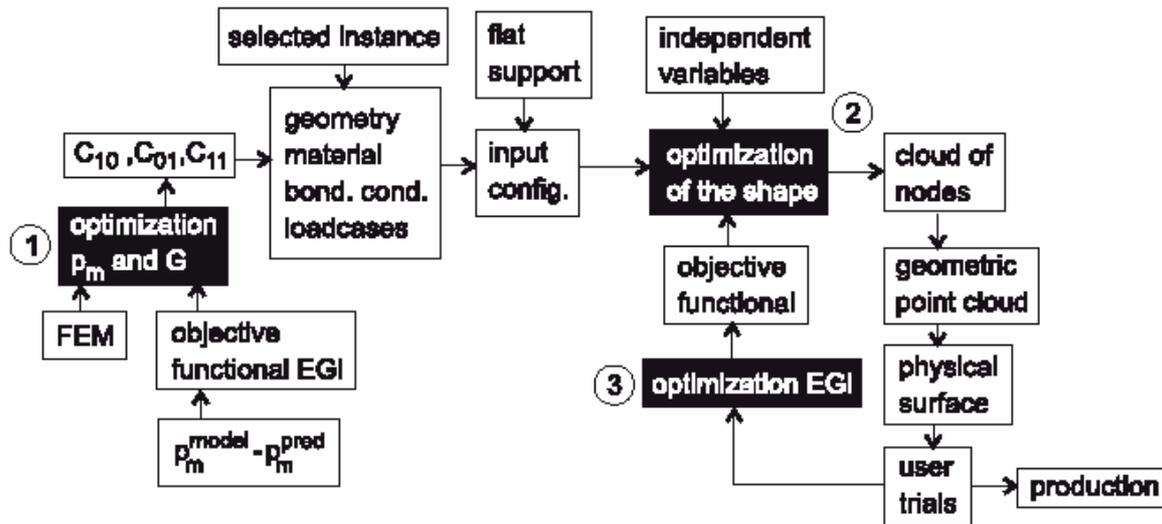

Figure 2. Overview of the procedures to conceptualize the ergonomics optimized shape

Figure 2 gives an overview of the complete set of procedures, where the optimizations are shaded. The first concerns the material properties of the skin and soft tissue; because large deformations are ex-pected, the material properties are defined non-linear. The second is the actual shape optimization. The third concerns the quantification of e. The e can be elaborated and optimized when more knowledge is gained about the main factors that contribute to the pressure distribution; later it will be applied to define e for different product types, types of usage, etc. Eventually the last optimization will be the very core of this research project. This paper describes the first optimization: the optimizatio of the material properties.

Several investigations on the non-linear elastic behaviour of living tissue were reported [Vannah & Childress 1996; Steege & Childress 1988; Azar et al. 2000; Nakamura et al. 1981]. The results relate to the first two or three coefficients of the 5-term James-Green-Simpson strain energy model for incompressible materials.

$$W = C_{10}(I_1 - 1) + C_{01}(I_2 - 1) + C_{10}(I_1 - 1)C_{01}(I_2 - 1) + C_{20}(I_1 - 1)^2 + C_{30}(I_1 - 1)^3$$

where W is the strain energy, I_1 and I_2 the strain invariants, and C_i the coefficients that determine thestiffness of the material [MARC 2000]. The range of their experimental setup and the corresponding results gave no indication of a usefull denominator.

To find a valid estimation of the elastic properties of the skin and the soft tissue several approaches can be followed. Two will be mentioned. The coefficients are found by fitting the derivative of the strain energy-function, which gives the stress-strain relationship, to experimental stress-strain data. These data can be obtained from in vivo experiments or from excised specimens. [Vannah & Childress 1996] determined $\{C_{10}, C_{01}, C_{11}\}$ and applied them to a Finite Elements Model, but no experimental

MULTIDISCIPLINARY ASPECTS OF DESIGN

verification was done to see if the resulting pressure distribution of the loaded Finite Elements Model corresponds with experimentally obtained pressure distribution patterns. Another way is to compare indirect quant-ities such as the pressure distribution in the contact area obtained from FE analysis with the pressure distribution obtained from experiments. Then the material coefficients can be varied for optimum corelation. This way was chosen for the current research. Experimental data are available [Moes 2000c; Moes 2000a].

2. Reasoning model

The basic idea to find an estimation of the material properties of the upper leg and buttock area that give under a flat and horizontal load a pressure distribution that corresponds with the predicted pressure distribution is as follows. First, a Finite Elements Model is created with geometric features that agree with a real subject. Second, for this subject the main pressure distribution parameters are estimated by known predictive relationships. The third step is the optimization. The load is iteratively applied on the Finite Elements Model, and the pressure distribution parameters are calculated for varying material properties until the calculated pressure distribution matches the predicted pressure distribution.
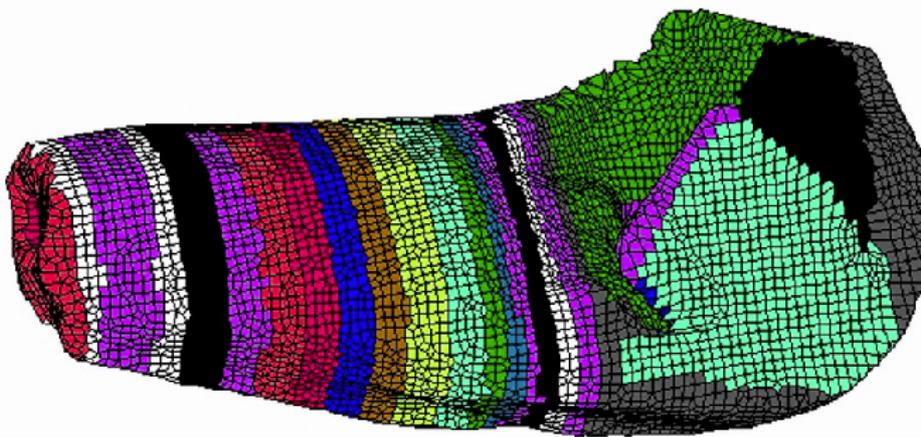

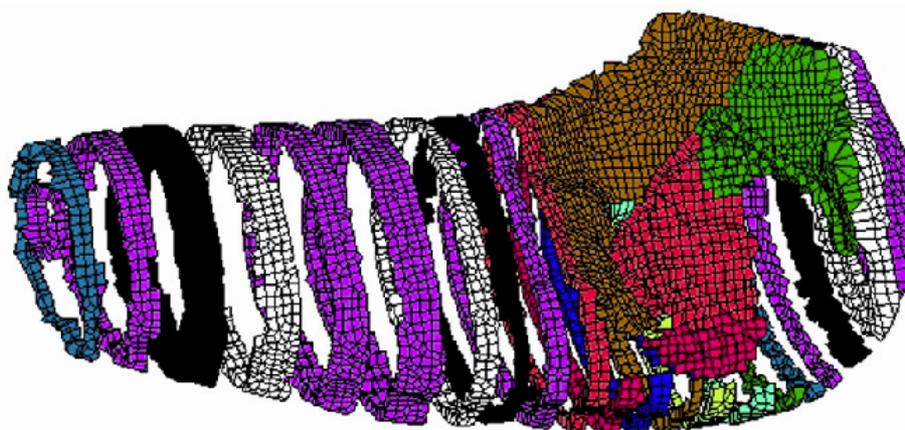**Figure 3. Medio-lateral view of the hexmeshed finite elements model**

Figure 4. View of a part of the model elements: a part of the skin, the most caudal ring of the femur, the seating bone, the sacrum, a part of the pelvis, and the auxillary surface to connect the skin and the pelvis bones
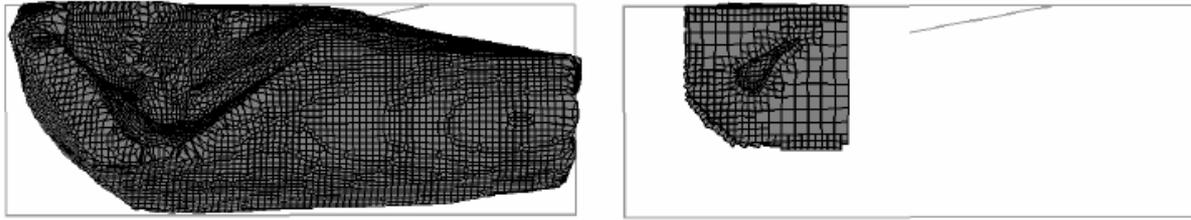
Figure 5. Topview of the rigid surface (seat) and the deformable body. The left figure shows the complete model. The right figure shows the reduced model

2.1 Finite Elements Model

Human skin and subcutaneous tissues consist of several components such as fat, muscle tissue, skin layers, tendinous structures and blood vessels. Most of these tissues are surrounded by or contain fluid elements such as blood, interstitial fluid and lymph. Consequently an advanced FE model should take the *viscous* effects into account. [Bogen 1987] argued that since human tissue is 80% water, important properties are obscured if such tissue is treated as 'solid'.

To have the model managable in the current state of the research such properties were neglected. The current Finite Elements Model reflects only three components of the body: the skin, the bony tissue, and a matrix of soft tissue. The bony tissue was considered undeformable. Between the skin and the bony tissue exists only isotropic, non-viscous, non-creep soft tissue. The hip joint and the sacro-iliac joint have no freedom of movement.

A closed FE *surface* model was generated for a 'statistical' male subject, body mass 77 kg, and ectomorphic index 6. This model was derived from geometric models of a few body parts. (i) The skin of the upper leg and the buttock area. These were measured for a living subject. The location of a set of bony landmarks was also measured that serve as register points for the bony parts to be included later. (ii) The bony parts including the femur, the pelvis and the sacrum. These were obtained from the male Visible Human Data set [VHP 1997].

Fitting the bones within the skin shape was done using the measured location of specific landmarks of the subject, followed by translation, rotation and scaling of the bone geometries [Moes et al. 2001]. The surface model was then converted to a solid model of hexagonal elements. The bulk mass of the solid model was defined as a matrix of isotropic, homogeneous soft tissue between skin and bone. Figure 3 shows the complete model in a medio-lateral view. Figure 4 shows the same model, but here a number of elements has been removed to have a view in the inner structure of the model. A second body was defined for the supporting surface (the chair). This was a geometric flat, horizontal (x - y plane) surface initially positioned below the deformable Finite Elements Model. This surface is shown as the rectangle in the left figure 5. During the zero-th increment this surface was moved in the z directionuntil contact with the deformable body was detected. Then the actual load was applied.

2.2 Predicted pressure distribution

In [Moes 2000a] the maximum pressure in the contact area and the sitting force are predicted for specific body characteristics. For the maximum pressure $p_{max} = 3.86 + 4.22 \, x \, ecto \, N / cm^2$, where *ecto* is the ectomorphic index, and the sitting force $F_s = 25.5 + 7.98 \cdot m$ N, so that for our subject the maximum pressure equals $29.18 \, N / cm^2$ or 292 kPa, and the sitting force 589 N.

2.3 Optimization

The loading force equals half of the sitting force. After applying this load the contact area becomes a flat surface. The main characteristics of the resulting pressure distribution in the contact area are the maximum pressure over the ischial tuberosity area, the pressure gradient, the magnitude of the contactarea, the location of the maximum pressure points,and the average pressure [Moes 2002b], but only the maximum pressure will be evaluated in this optimization.
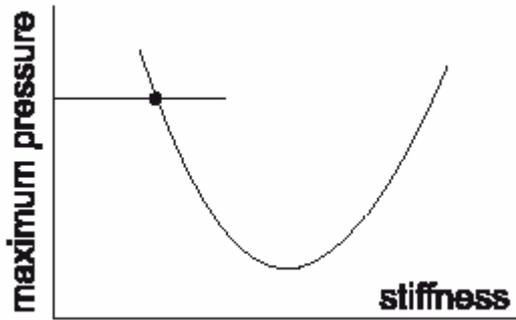
MULTIDISCIPLINARY ASPECTS OF DESIGN

Figure 6. The assumed relationship of the maximum pressure and the material stiffness

Now consider a FE model that is loaded by the sup-port. It was assumed that the maximum pressure at the interface depends on the stiffness of the tissue. For *high* values of the stiffness the body shows little deformation so that the sitting force is distributed over a relatively small contact area, so that the maximum contact pressure is high, and shows no relationship with the shape of the ischialtuberosities. For decreasing stiffness the contact area increases, and the maximum pressure decreases. For very *low* stiffness the body is impressed quickly and the maximum pressure is caused by extremely decreased distance between the lower aspect of the ischial tuberosity and the buttock skin surface. Now the shape of the ischial tuberosity is the main factor that determines the location and the magnitude of the maximum pressure. The location of the maximum pressure points for high and low stiffness are possibly different. Figure 6 visualizes the relationship. The horizontal line is the predicted pressure, and the big dot marks the point to search for. It is assumed that the re-lationship shows a minimum. From observation it is expected that the maximum pressure is located at the left, decreasing part of the graph. The goal of this research is (i) to confirm the behaviour as it is shown in figure 6 (ii) to find the stiffness that gives a value of the maximum pressure corresponding with the predicted value. The next step is to optimize the maximum pressure and the pressure gradient simultaneously.

2.4 Material properties

The expected deformations are large so that non-linear elasticity must be applied. Since human tissues contain mainly water, incompressibility was assumed. Most reports on the non-linear, mechanical properties of living tissue describe the deformation by the strain invariants $I_1 = l_1^2 + l_2^2 + l_3^2$, $I_2 = l_1 l_2 + l_2 l_3 + l_3 l_1$ where $l_i = (l_i + \Delta l_i)/l_i$ are the principle stretch ratios. The third invari-ant, $I_3 = l_1 l_2 l_3 = 1$ because of incompressibility. Finite elements solvers balance the internal strain energy with the applied external forces. The calculation of the strain energy depends on the differential elasticity and the strain. Most models form a subset of the third order James-Green-Simpson deformation formulation

$$W = C_{10}(I_1 - 3) + C_{01}(I_2 - 3) + C_{11}(I_1 - 3)(I_2 - 3) + C_{20}(I_1 - 3)^2 + C_{30}(I_1 - 3)^3$$

[MARC 2000]. For compression of living tissue [Vannah & Childress 1996] showed that the first threeterms are sufficient. Since experimental stress strain curves are not available for the involved bodyparts their results were used as initial values for the search. The ratio of the coefficients was set to $C_{10} = 4C_{01} = 0.5C_{11}$. Currently the soft tissue was assigned the same material properties as the skin, but in coming experiments the two tissues will be distinguished. First trials only the first coefficient, which represents the neo-Hookean elastic behaviour. The initial value $C_{10} = 100$ kPa. Which is based on a simple, unreported experiment where the skin was impressed 1 cm by a square of 1 cm^2. This required a load of approximately 1 N. This turned to be unsufficient for the lower stiffness values, since the elements showed already after a small pressure a negative third invariant (negative volume). Using the first two coefficients gives the Mooney-Rivlin model, often applied for soft rubber materials. An inprovement was reached for the low stiffness range. The last experiments reported here were done with the three-term model.

2.5 Boundary conditions

To simulate the assumptions that the bony parts are practically undeformable and that the hip joint is fixed, the bony 'substances' were removed from the model. The surface nodes, that now form the inner closure of the body, were fixed in space. The original geometric measurements and the construction of the model is discussed in detail in [Moes 2002a].

The boundary conditions for the deformable body include the fixed spatial positions of the bonenodes, the reduced freedom of movement of some boundary surfaces to simulate body symmetry or tissue continuation. Since the material properties are non-linear the load is applied in a series of incre-ments.

2.6 Practical limitations

Pilot studies showed that hardware limitations required a size reduction. In the current stage of the project this does not pose a serious problem since it still carries the character of a feasibility study. The complete soled Finite Elements Model consists of ca. 30,000 elements. It requires more than 20 Gb working memory. The reduced model has ca. 2300 elements and works with the available amount of 850 Mb. In the left figure 5 the reduced model is shown.

3. Results

The maximum pressure in the contact area was represented by the Cauchy(33) component, s_{33}. First experiments were done with the two parameter model, with $C_{01} = 1/2 \, C_{10}$. Above $C_{10} = 4 \, \text{kPa}$ the model was stable. But for lower values the model increasingly showed instabilities, mainly caused by (i) slow convergency, (ii) singular element matrix, and (iii) body to body contact. The upper part of table 1 and the black squares in figure 7 summarize the relationship between s_{33} and C_{10}. The number of recycles to obtain convergency and the cpu-time needed are given in the second and the third column. The last two columns give s_{33} and the maximum displacement of the support. It is clear that the search procedure can not be carried out based on these data.

Table 1. The results of the FEA for two and for three coefficients

| C_{10} kPa	cycles	time hr	σ_{33} kPa	impress mm
two-coefficient approach				
2.5	1479	48.8	19.0	27.2
3.0	577	21.5	22.2	26.8
4.0	460	14.4	27.5	24.9
5.0	457	13.9	31.3	23.0
10.0	356	11.5	50.7	17.6
20.0	300	8.8	14.0	9.3
three-coefficient approach				
0.5	445	14.5	29.9	32.1
1.0	356	13.1	27.2	28.6
1.5	367	11.0	30.5	26.5
2.0	352	11.1	33.4	24.9
2.5	378	12.0	36.8	22.5
3.0	387	12.5	40.6	22.6
4.0	396	12.8	46.7	21.0
5.0	383	13.4	51.9	19.7
10.0	375	11.3	75.5	16.0
20.0	365	11.3	123.5	12.6
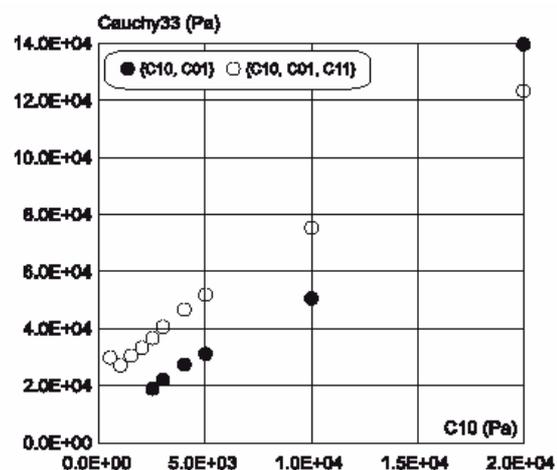
Figure 7. The relationship between the maximum pressure, the maximum displacement of the support, and the elasticity. The black squares show the res-ults of the two-coefficient analysis; the circles give the displacement and the maximum pressure of the three-coefficient analysis

Therefore another analysis was done with the three-coefficient model. The value of C_{11} was twice C_{10}, so that $C_{10} = 4C_{01} = C_{11}/2$. The analysis was stable for values as low as $C_{10} = 500$ Pa. The results are summarized in the lower part of table 1; see also the black circles in figure 7. For this definition of the elasticity a minimum of the assumed function was suggested by the increase of s_{33} for C_{10} running from 1 kPa to 500 Pa. However, for lower values the time step became so small that further analysis was not possible. The open circles give the displacement of the support from the point of initial contact until maximum applied load (300 N) for the three coefficient analysis.

4. Discussion and conclusions

For the applied range of elasticity definitions the left part of the curve of figure 6 could not be confirmed. Therefore with the current setup it is not yet possible to obtain the value of $\{C_{10}, C_{01}, C_{11}\}$ that matches the maximum pressure of the FE model with the predicted maximum pressure from the regression equations. Some assumptions done in the setup procedures could account for this.

Although the geometry of the bony parts was carefully scaled and positioned within the shape of the skin, these geometries stem nevertheless from different subjects. Thus the shape of the ischial tuberosities can show different curvatures. Moreover, it was assumed that in the upright sitting posture the angle of the plane through the upper front edge of the pubis and the two SIASes[1] has an backward inclination of 30° with respect to the (horizontal) femur. A deviation implies that a different part of the ischial tuberosity causes the maximum pressure.

The predicted pressure distribution pattern describes one pressure mountain with a predicted loca-tion, maximum pressure and pressure gradient, which agrees with the observed measured patterns [Moes 2002b]. A typical surface pressure distribution pattern resulting from the FEA is presented in the left figure 8, showing several maxima. The right figure 8 shows a typical stress distribution in a vertical cutting plane along the length of the ischium. The highest values of the stress were not found at the surface but within the tissue, close to the bone boundary. This is not surprising since in medical practice it is known that decubitus ulcers in the sitting region never start at the surface of the skin, but close to the bony area, then extending in time towards the surface of the buttocks.
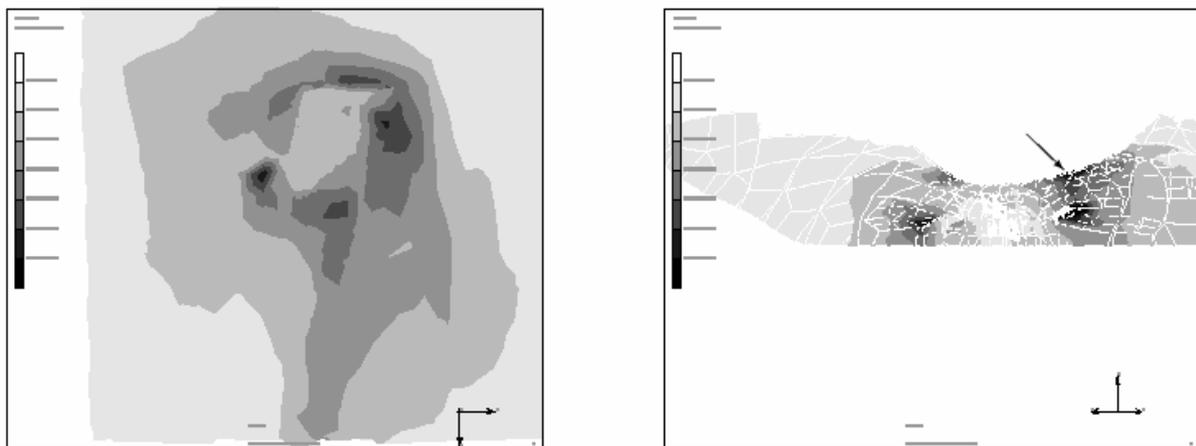

Figure 8. The left figure shows a typical pressure distribution pattern. for $C_{10} = 500$ Pa and maximum load. The right figure shows a typical stress (s_{33}) pattern in a vertical cutting plane along the length of the ischium

---

[1] upper superior iliac spine.

It was surprising that for very small C_{10} the maximum stress did not happen below the lowest (z) part of the seating bone, see the arrow in the right figure 8. This can be understood by considering the shape of this bone. The lowest part has a larger radius of curvature. In forward direction the radius decreases, resulting in a 'sharper' bone, where the stresses are more concentrated on a smaller area. Further research is needed.

The phenomenon of the unexpected stress behaviour inside the tissue is possibly a consequence of the applied mesh generation procedure. Since the force is transmitted via the nodes they should ideally be positioned along along the pressure gradient curves, see figure 9. This was not controlled during the automatic generation of the hexagonal elements. One consequence was the necessity of adaptive remeshing, which appeared to unsufficiently compensate for this mistake.
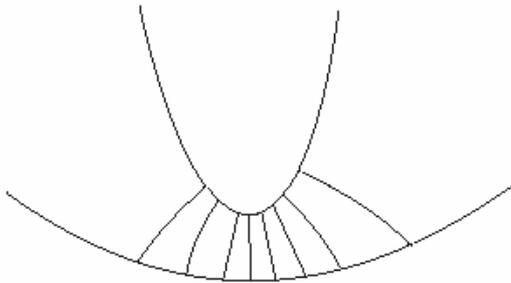

Figure 9. Geometric curves running from the ischium to the skin surface along expected pressure gradient curves

In the past, models were developed for artificial, rotationsymmetric geometry fullfilling this condition auto-matically[Chow & Odell 1978]. Also the model of [Todd & Tacker 1994] showed more or less such arrangement.Although it is unknown how human tissue behaves under large deformation, the material properties were defined by a linear combination of the deformation invariants for in-compressible, non-viscous, non-plastic, and purely elastic materials. Pilot analyses showed that the neo-Hookean model was not adequate for large compression; crossing element boundaries could not be avoided resulting in pre-mature program ending. With the Mooney model it was not possible to obtain convergency for lower levels of the elasticity, which resulted in numerous force cut-backs and reduction of the time step to machine inaccuracy. The three coefficient James-Green-Simpson formulation allowed lower values of C_{10} then the two coefficient model, but the searched forincrease of the maximum pressure could not be obtained either.

In the real human body several different tissues exist, each with its specific, usually anisotropic, material properties. In the current model, however, only soft tissue and skin were modelled, while the skin was attributed with the same material properties as the soft tissue.

Further research must shine its light on the following questions.

- Although the assumed material model can be fitted to compressive stress-strain measurement data, resulting in an estimate of {C 10 C +01 ,C 11 }, it must be done for more regions of the body. It is, for instance, expected that the stiffness in the buttock area is different from the upper leg area.
- Knowing the coefficients for the different body regions, it is still questionable if such description of the elasticity is adequate to describe the 3D stress-strain behaviour, and if it leads to the correct interface pressure distribution that considers a larger region around the maximum pressure points.
- If this approach gives reasonably good results the second optimization procedure of should enable the optimization of the coefficients.

An improved model is currently being build that includes the following features. (i) A skin layer of 3 mm constant thickness [Moes 2000b]. (ii) Mesh generation control for the location of nodes along the expected pressure gradient curves. (iii) Reconsidered position of the bony pelvis with respect to the skin surface. Ideally the bony shape should be obtained for a specific subject by MRI-scanning.

References

Azar FS, Metaxas DN, Miller RT, & Schnall MD Methods for Predicting Mechanical Deformations in the Breast During Clinical Breast Biopsy In Proceedings of the 26th IEEE Northeast Bioengineering Conference, 2000 pp.
Bogen DK Strain Energy Descriptions of Biological Swelling I: Single Fluid Compartment Models J of Biomechanical Engin Vol. 109, 1987, pp. 252–256

Chow WW & Odell EI Deformations and Stresses in Soft Body Tissues of a Sitting Person Journal of Biomedical Engineering Vol. 100(may), 1978, pp. 79–87

Horv´ath I, 1998 Shifting Paradigms of Computer Aided Design Delft University of Technology,Faculty of Industrial Design Engineering Inaugural Speech

MARC, 2000 MSC.Marc Advanced Course Course material MSC Software, Munchen, Germany

Moes CCM Distance Between the Points of Maximum Pressure for Sitting Subjects In Proceedings of the 6th International Design Conference DESIGN2000, 2000 pp. 227–232

Moes CCM Geometric Model of the Human Body In Proceedings of the TMCE2000, 2000 pp. 79–92

Moes CCM Pressure Distribution and Ergonomics Shape Conceptualization In Proceedings of the 6th International Design Conference DESIGN2000, 2000 pp. 233–240

Moes CCM Estimation of the Nonlinear Material Properties for a Finite Elements Model of the Human Body In Proceedings of the TMCE2002, 2002 Status: accepted for publication

Moes CCM Modelling the Sitting Pressure Distribution and the Location of the Points of Maximum Pressure for Body Characteristics and Rotation of the Pelvis Ergonomics Vol. ?, 2002

Moes CCM, Rus´ak Z, & Horv´ath I Application of vague geometric representation for shape instance generation of the human body In Proceedings of DETC'01, Computers and Information in Engineering Conference, 2001 pp. (CDROM:DETC2001/CIE–21298)

Nakamura S, Crowninshield RD, & Cooper RR An Analysis of Soft Tissue Loading in the Foot – A Preliminary Report Bull. of Prosth. Res.Vol. 18 (10-35), No. 1, 1981, pp. 27–34

Steege JW & Childress DS Finite Element Modeling of the Below-Knee Socket and Limb: Phase II In ASME Modelling and Control Issues in Biomechanical Systems volume BED-4, 1988 pp. 121–129

Todd BA & Tacker JG Three-dimensional computer model of the human buttocks, in vivo Journal of Rehabilitation Research and Development Vol. 31, No. 2, 1994, pp. 111–119

Vannah WM & Childress DS Indentor tests and finite element modeling of bulk muscular tissue in vivo J. of Rehab. Res. and Devel.Vol. 33, No. 3, 1996, pp. 239–252

VHP, 1997 The Visible Human Project URL: http://www.nlm.nih.gov/research/visible/visible – human.html

Niels C.C.M. Moes, MSc
Delft University of Technology, dept of Industrial
Design Engineering
Landbergstraat 15, 2628 CE Delft, the Netherlands
Telephone (31)15 278 3006
Telefax(31)15 278 7316
E-mail C.C.M.Moes@IO.TUDelft.nl